

SYNTHESIS AND CHARACTERIZATION OF SrF₂ AND SrF₂:Ce³⁺ NANOPARTICLES FOR GAMMA RAY DETECTION

Erhan AKSU¹, Haydar DİŞBUDAK², Selen Nimet GÜRBÜZ GÜNER³, Mahmut EKEN⁴, Ece ERGUN⁵, Yücel Özer ÖZKÖK⁶ and Ömer GÜNDÜZ⁷

- 1- Türkiye Atom Enerjisi Kurumu Sarayköy Nükleer Araştırma ve Eğitim Merkezi, Kahramankazan, Ankara, Türkiye, 06983, +90 312 810 1708, erhan.aksu@taek.gov.tr
- 2- Türkiye Atom Enerjisi Kurumu Sarayköy Nükleer Araştırma ve Eğitim Merkezi, Kahramankazan, Ankara, Türkiye, 06983, +90 312 810 1807, haydar.disbudak@taek.gov.tr
- 3- Türkiye Atom Enerjisi Kurumu Sarayköy Nükleer Araştırma ve Eğitim Merkezi, Kahramankazan, Ankara, Türkiye, 06983, , +90 312 810 1650, selen.gurbuz@taek.gov.tr
- 4- Türkiye Atom Enerjisi Kurumu Sarayköy Nükleer Araştırma ve Eğitim Merkezi, Kahramankazan, Ankara, Türkiye, 06983, , +90 312 810 1807, mahmut.eken@taek.gov.tr
- 5- Türkiye Atom Enerjisi Kurumu Sarayköy Nükleer Araştırma ve Eğitim Merkezi, Kahramankazan, Ankara, Türkiye, 06983, , +90 312 810 1591, ece.ergun@taek.gov.tr
- 6- Türkiye Atom Enerjisi Kurumu Sarayköy Nükleer Araştırma ve Eğitim Merkezi, Kahramankazan, Ankara, Türkiye, 06983, , +90 312 810 1620, yucel.ozkok@taek.gov.tr
- 7- Türkiye Atom Enerjisi Kurumu, Sarayköy Nükleer Araştırma ve Eğitim Merkezi, Kahramankazan, Ankara, Türkiye, 06510, , +90 312 810 1715, omer.gunduz@taek.gov.tr

GAMA IŞINLARININ TESPİTİNDE KULLANILMAK ÜZERE SrF₂ VE SrF₂:Ce³⁺ NANO PARTİKÜLLERİNİN SENTEZLENMESİ VE KARAKTERİZASYONU

Özet

SrF₂ ve SrF₂:xCe³⁺ (x=0.5 mol %, 0.6282 g -10 mol %, 12.5630 g) nanoparçacıklar kimyasal birlikte çöktürme yöntemiyle sentezlenmiştir. Katkısız ve seryum katkılı nanoparçacıkların yapısal ve optik özellikleri X-Işını Difraktometresi (XRD), Yüksek Çözünürlüklü Geçirimli Elektron Mikroskobu (HRTEM) ve Fotoluminesans Spektrofotometre (PL) ile karakterize edilmiştir. Sentezlenen nanoparçacıkların ortalama parçacık boyutları, Debye-Scherrer eşitliği kullanılarak, X-Işını kırınım desenlerindeki piklerin genişlemesinden belirlenmiştir. Hesaplanan ortalama parçacık boyutları 30 nm - 52 nm aralığında değişmektedir. Sentezlenen tüm nanoparçacıkların uyarma ve emisyon piklerinin dalga boyları sırasıyla 232 nm ve 464 nm'dir. Disk şekline sahip iri ve hacimli nanokompozit sintilatör malzemelerin üretiminde sentezlenen SrF₂ and SrF₂: %1 Ce³⁺ nanoparçacıklar fosfor dolgu malzemesi olarak, epoksi reçine ise matriks malzemesi olarak kullanılmıştır. Üretilen iri ve hacimli nanokompozit sintilatör malzemelerinin enerji spektrumları Am-241, Cs-137 ve Co-60 nokta kaynakları kullanılarak elde edilmiştir. Elde edilen spektrumlar incelendiğinde üretilen nanokompozit sintilatör malzemelerin, gama ışını dedeksiyonunun yanı sıra, gelen gama ışınının enerjisini ayırabilecek potansiyelde olduğunu göstermektedir.

Abstract

SrF₂ and SrF₂:xCe³⁺ (x=0.5 mol %, 0.6282 g -10 mol %, 12.5630 g) nanoparticles were synthesized using chemical co-precipitation method. Structural and optical properties of the undoped and cerium doped nanoparticles were characterized with X-Ray Diffraction (XRD), High-Resolution Transmission Electron Microscopy (HRTEM), and Photoluminescence (PL)

Spectroscopy. Average sizes of the synthesized nanoparticles were determined from the broadening of X-Ray Diffraction peaks using Debye-Scherrer equation. Calculated values were ranging between 30 nm-52 nm. All synthesized nanoparticles show photoluminescence characteristics with an excitation and emission peaks centered at 232 nm and 464 nm, respectively. Disc shaped bulk nanocomposite scintillators were also fabricated using synthesized SrF_2 and $\text{SrF}_2:1\% \text{Ce}^{3+}$ nanoparticles as phosphor fillers and epoxy resin as matrix material. Energy spectrums of bulk nanocomposite scintillators were obtained using Am-241, Cs-137, and Co-60 point sources. Gamma ray energy responses of the fabricated scintillator materials revealed the fact that, beside the detection of gamma ray, these nanocomposites have a potential for energy discrimination of the incoming ray.

Anahtar Kelimeler: Seryum katkılı stronsiyum florür ($\text{SrF}_2:\text{xCe}$), gama spektroskopisi, gama ışını dedeksiyonu, nanokompozit sintilatör, stronsiyum florür (SrF_2).

Keywords: Cerium doped strontium fluoride ($\text{SrF}_2:\text{xCe}$), gamma spectroscopy, gamma ray detection, nanocomposite scintillator, strontium fluoride (SrF_2).

1. Introduction

Inorganic scintillator materials are commonly used to detect ionizing radiation. Beside radiation detection, these materials also find application in several areas such as medical imaging, high energy physics, oil exploration, homeland security, and etc. (Canning, Chaudhry, Boutchko and Gronbech-Jensen, 2010). Currently, single crystal inorganic scintillators such as NaI:Tl, CsI:Na, LaBr₃:Ce single crystals are widely used for the detection of ionizing radiation. However, operation and maintenance of these high performance single crystal scintillators are difficult and expensive. Therefore, in recent years, studies have focused on the investigation of high performance new composite scintillator materials that are low cost, easy to manufacture and maintenance (De Haas and Dorenbos, 2008; Rogers, Han, Wagner, Nadler and Kang, 2011; Guss, Guise, Yuan, Mukhopadhyay, O'Brien, Lowe, Kang, Menkara and Nagarkar, 2013).

SrF_2 scintillator material is one of such promising scintillator material because of its wide band gap, high radiation resistance, low photon energy and low refraction index along with high mechanical strength (Yagoub, Swart, Noto, Bergman and Coetsee, 2015). On this account, characterization and fabrication of SrF_2 scintillator materials doped with lanthanide elements has been the focus of intense research for decade (Yagoub, Swart, Noto, Bergman and Coetsee, 2015; Jin, Qin and Zhang, 2008; Shendrik, Radzhabov and Nepomnyashchikh, 2013; Shendrik and Radzhabov, 2012; Shendrik and Radzhabov, 2010). These studies mainly concentrated on the fabrication of lanthanide doped SrF_2 single crystals (Shendrik, Radzhabov and Nepomnyashchikh, 2013; Shendrik and Radzhabov, 2012; Shendrik and Radzhabov, 2010) and, as far as author knows, the researches that focused on the synthesis of lanthanide doped SrF_2 nanoparticles are limited (Yagoub, Swart, Noto, Bergman and Coetsee, 2015; Jin, Qin and Zhang, 2008). Shendrik et al. studied the production and characterization of SrF_2 single crystal doped with lanthanides for the use as gamma ray detector (Shendrik, Radzhabov and Nepomnyashchikh, 2013; Shendrik and Radzhabov, 2012; Shendrik and Radzhabov, 2010). In these studies, SrF_2 single crystal doped with either Ce^{3+} or Pr^{3+} lanthanides were prepared using Stockbarger method and light yield measurements were performed. The light output of the prepared 0.3% Ce^{3+} doped SrF_2 single crystal was reported as 33970 photons per MeV where the light output of NaI:Tl single crystal gamma ray detector was reported as 43000 photons per MeV (Shendrik, Radzhabov and Nepomnyashchikh, 2013).

On the other hand, Yagoub et al. (2015) and Jin et al. (2008) synthesized SrF₂ nanophosphors doped with lanthanide elements using hydrothermal method (Yagoub, Swart, Noto, Bergman and Coetsee, 2015; Jin, Qin and Zhang, 2008). Jin et al. (2008) synthesized 50 nm sized SrF₂:Eu³⁺ nanoparticles whereas Yagoub et al. (2015) used Ce beside Eu as dopant and synthesized SrF₂:Ce³⁺ and SrF₂: Eu, Ce³⁺ nanoparticles. In these studies, structural and luminescent properties were characterized, but the gamma ray energy response of the synthesized nanoparticles was not investigated (Yagoub, Swart, Noto, Bergman and Coetsee, 2015; Jin, Qin and Zhang, 2008).

In the scope of this study, SrF₂ and SrF₂:xCe³⁺ nanoparticles were synthesized using chemical co-precipitation method. Structural and optical properties of the undoped and cerium doped nanoparticles were characterized with X-Ray Diffraction (XRD), High-Resolution Transmission Electron Microscopy (HRTEM), and Photoluminescence (PL) measurements. In order to investigate the gamma ray energy response, synthesized nanoparticles were incorporated into epoxy (EPOTEK-301-2FL) matrix and gamma ray energy spectrums of these composite scintillators were obtained.

2. Materials and Methods

2.1 Materials

For the synthesis of nanoparticles, used chemicals were NaF (99.9%, Merck), Oleic Acid (90%, Aldrich), Sr(NO₃)₂ (98%, Fluka), Ce(NO₃)₃.6H₂O (99.9%, Aldrich), and Ethyl Alcohol (99.8%, Aldrich). All these chemicals were reagent grade and used without further purification.

2.2 Synthesis of SrF₂ and SrF₂:xCe³⁺ Nanoparticles

SrF₂ and SrF₂:xCe³⁺ (x=0.5%, 1.0%, 2.0%, 5.0%, 10.0%) nanoparticles were synthesized using chemical co-precipitation method. The synthesis procedure was adapted from the study of Rogers et al. (Rogers, Han, Wagner, Nadler and Kang, 2011) and here, details of the synthesis procedure will be mentioned only for SrF₂ nanoparticles doped with 1% Ce³⁺. Aqueous solution of NaF was prepared by dissolving 2.1334 g (0.05 mole) NaF in 133 mL de-ionized water. Solution of oleic acid (OA)-ethyl alcohol was prepared by adding 4.8 g OA (0.017 mole) to 133 mL ethyl alcohol and stirred. Aqueous solution of NaF was mixed with OA-ethyl alcohol solution in a flask. While stirring with a magnetic stirrer, the temperature of the mixture was raised to 78°C. Then, aqueous solution of Sr(NO₃)₂ and Ce(NO₃)₃.6H₂O was prepared by dissolving 5.326 g (0.025 mole) Sr(NO₃)₂ and 0.1104 g (2.54x10⁻⁴ mole) Ce(NO₃)₃.6H₂O in 53 ml de-ionized water. Following, this prepared aqueous solution was added drop-wise via a peristaltic pump to NaF-OA solution while stirring at 78°C. The dropping speed was kept low and the total dropping time was 20-30 min. After addition of the prepared aqueous solution, the mixture was kept at 78°C for another 1 hr. under constant stirring and left to cool to room temperature. Formed white precipitate was separated by decantation. In order to remove residue of OA and inorganic salts, white precipitate was washed sequentially with ethyl alcohol and de-ionized water for three times using ultrasonic bath. After each washing step, the mixture was subjected to centrifugation at 3000 rpm for 15 min. Synthesized nanoparticles were dried in a drying oven at 30 °C under the vacuum.

2.3 Fabrication of Nanocomposite Scintillators

Nanocomposite scintillator samples were prepared using SrF₂ and SrF₂:1%Ce³⁺ nanoparticles as phosphor fillers. After mixing the epoxy resin (EPO-TEK-301-2FL) and hardener according to the ratios suggested by the manufacturer, 5 wt% nanoparticles were

mixed with the epoxy resin system until a homogeneous mixture was obtained. The mixture was then poured into a cylindrical Teflon mold with a diameter of 32mm and a height of 50mm, respectively. In order to remove the entrapped air bubbles during mixing, the mixture was placed under vacuum. After subjecting to vacuum, the nanoparticle-epoxy mixture was placed in drying oven at 80°C for 3 hours to cure the epoxy matrix. Then, fabricated nanocomposite disc ($\phi=32\text{mm}$) with a thickness of 10 mm was removed from the mold. To obtain good surface finish, i.e. minimize surface scattering, surfaces of the fabricated composite samples were ground using SiC emery papers and then, polished down to 1 μm with diamond paste.

2.4 Characterization

Phase analysis of the synthesized nanoparticles were performed in the range of $2\theta=10^\circ-80^\circ$ with Bruker D8 Advance X-Ray Diffractometer ($\text{CuK}\alpha$ $\lambda=1.5405 \text{ \AA}$). High resolution transmission electron microscopy (HRTEM) images of the nanoparticles were collected by using JEOL 2100F HRTEM. For HRTEM imaging, synthesized nanoparticles were dispersed in toluene. Then, few drops of prepared nanoparticle-toluene suspension was dropped onto a grid, and allowed to dry at room temperature before examining with HRTEM.

For the Photoluminescence (PL) characterization, synthesized nanoparticles were dispersed in anhydrous methanol. Measurements were carried out using Varian Carry-Eclipse fluorescence spectrophotometer, equipped with a Xenon flash lamp using 2.5 nm slit widths. All measurements were carried out in quartz cells at room temperature.

Gamma ray energy spectrums of the fabricated nanocomposite scintillator samples were collected using photo multiplier tube (PMT) (ET Enterprises Ltd. Type: 9266KB50). These measurements were carried out using ORTEC digiBASE system and Maestro program. Before measurements, nanocomposite scintillator materials were coupled with PMT via optical grease. PMT-nanocomposite scintillator assembly was then optically shielded with black PVC tape. During measurements, point sources with different gamma-ray energies; Co-60, Cs-137, and Am-241, were directly placed on top of the disc shaped nanocomposite scintillator samples. The activities of the used Am-241, Cs-137, and Co-60 point sources were 1 μCi , 0.49 μCi , and 0.42 μCi , respectively.

3. Results and Discussion

X-ray diffraction patterns of the synthesized nanoparticles are shown in Figure 1. For all samples, XRD patterns were recorded in a 2θ range of $10^\circ-80^\circ$ and analyzed using the Diffplus-PDF2009.4CA database. All of the diffraction peaks, except one at $2\theta=45.656^\circ$, exactly matched with the characteristic peaks of cubic SrF_2 phase with a space group of $\text{Fm}\bar{3}\text{m}$ (225) (PDF card number: 086-2418). The presence of unidentified small peak at $2\theta=45.656^\circ$, seen in all diffraction patterns, is thought to be resulted from the impurities present in the raw materials used for the synthesis of the nanoparticles.

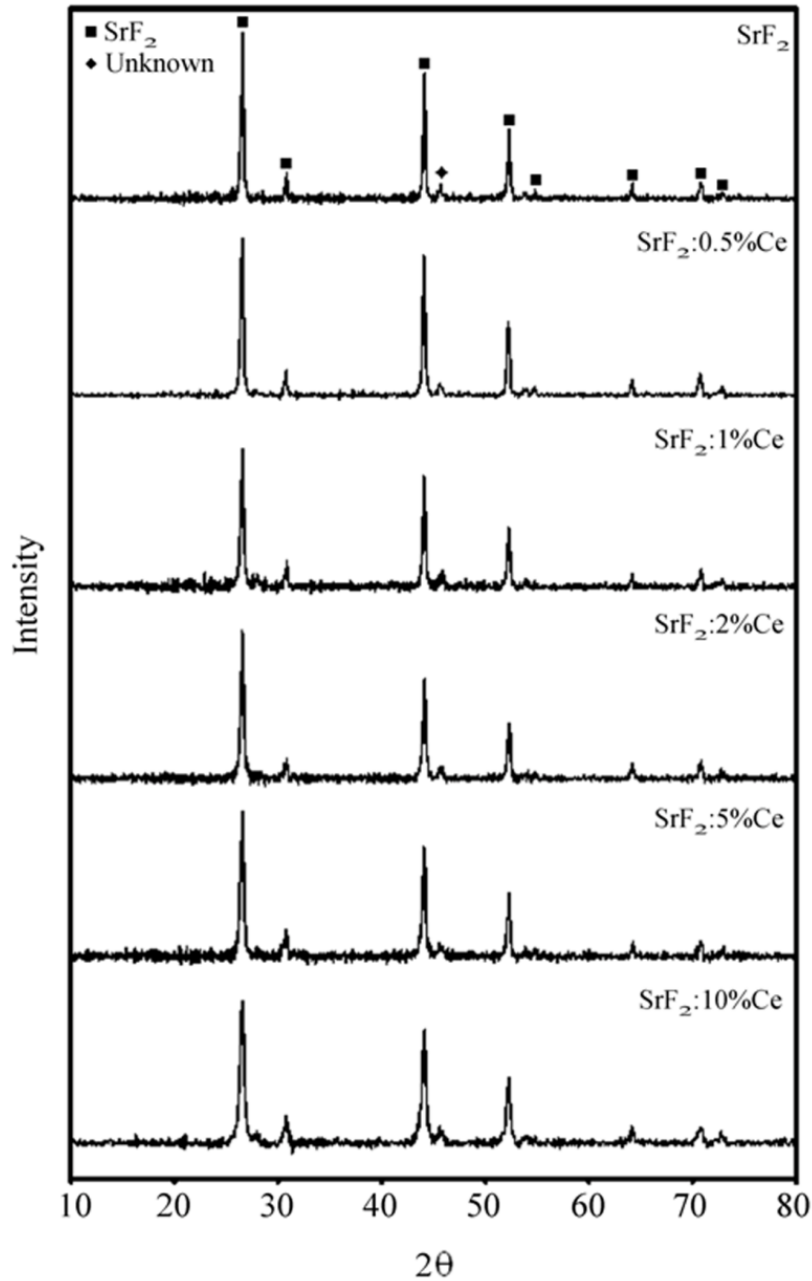


Figure 1. XRD patterns of synthesized SrF_2 and $\text{SrF}_2:\text{xCe}^{3+}$ ($\text{x}=0.5\%$, 1.0% , 2.0% , 5.0% , 10.0%) nanoparticles.

Figure 2 illustrates the HRTEM images of synthesized SrF_2 and $\text{SrF}_2:1\%\text{Ce}^{3+}$ nanoparticles. These images explicitly reveal that although the cuboidal-shaped particles are not uniform in size, they are all nanometer scale. However, particle aggregates, seen in HRTEM images, makes it difficult to estimate the average particle size. These particle aggregates are thought to be formed during sample preparation for HRTEM analysis.

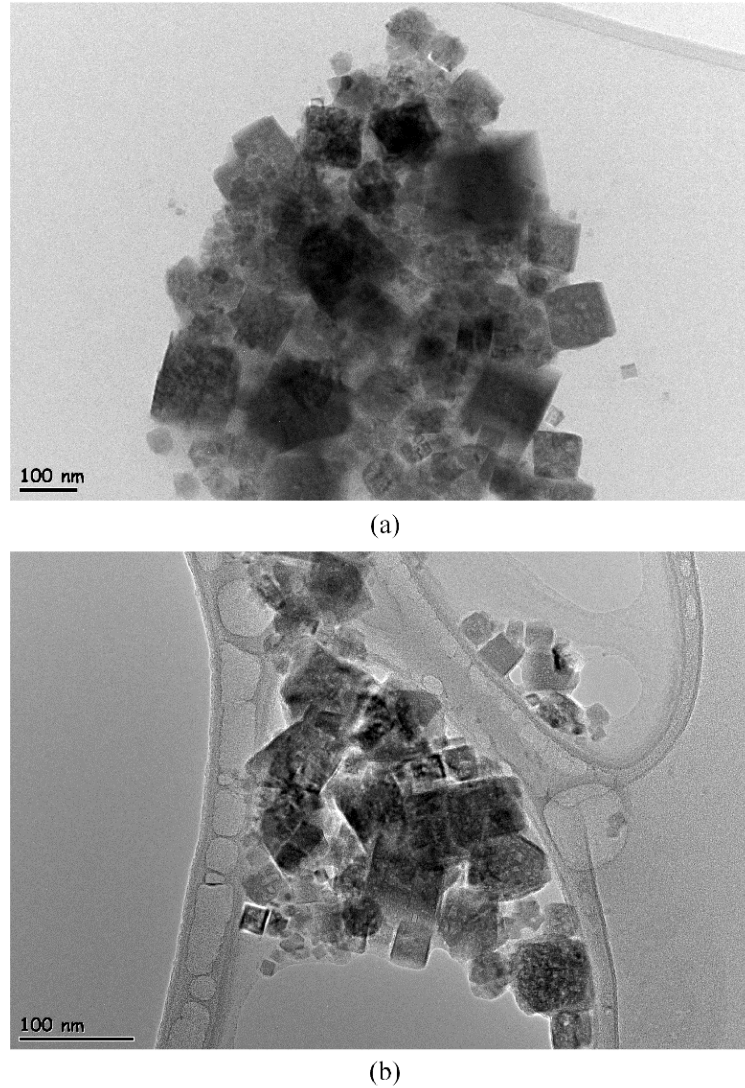


Figure 2. HRTEM images. (a) SrF₂ and (b) SrF₂:1% Ce³⁺ nanoparticles.

Therefore, average particle sizes of the synthesized nanoparticles were determined from widths of the six characteristic XRD peaks of the cubic SrF₂ phase by using Debby-Scherer equation (Patterson, 1939). These calculated values, presented in Table 1, were ranging between 30 nm-52 nm. Along with HRTEM images, these determined average particle size values indicate that nanoparticles of SrF₂ either undoped or doped with different amounts of Ce³⁺ were synthesized successfully by chemical co-precipitation method.

Table 1. Average sizes of the synthesized nanoparticles calculated using Debby-Scherer equation.

Average Particle Size (nm)	
SrF ₂	44.5

SrF ₂ :0.5%Ce	30.0
SrF ₂ :1%Ce	33.3
SrF ₂ :2%Ce	41.2
SrF ₂ :5%Ce	52.0
SrF ₂ :10%Ce	42.6

Figure 3 shows the emission spectra of SrF₂ and 0.5-10% SrF₂:Ce³⁺ doped nanoparticles dispersed in methanol solutions. The photoluminescence excitation peak was found to be at 232 nm where the maximum intensity in emission spectra observed at 464 nm for all nanoparticle samples. Similar spectral characteristics, i.e. excitation and emission peaks centered at 232 nm and 464 nm, respectively, imply that same luminescent mechanisms are operative for these nanoparticles. Nevertheless, increase in the concentration of Ce dopant up to 5% leads to an increase in the intensity of the PL emission peak with respect to that of the undoped SrF₂ nanoparticles, and the highest luminescence intensity is observed for SrF₂:1%Ce³⁺ and SrF₂:2%Ce³⁺ nanophosphors. However, further increase in Ce content leads to a decrease in PL intensity as compared to that of the undoped SrF₂ nanoparticles.

The optical properties of nanoparticles depend not only on the nanoparticle size but also on the technique of their preparation. PL emission peak for undoped SrF₂ nanoparticles is thought to be resulted from the operative trapping mechanisms, i.e. self-trapped excitons, hole or electron traps (Canning, Chaudhry, Boutchko and Gronbech-Jensen, 2010; Shendrik, Radzhabov and Nepomnyashchikh, 2013). As aforementioned, with Ce doping, these operating mechanisms do not quenched and vanished for Ce contents up to 5% but rather the intensity of PL emission peak increases with the increase in Ce concentration as a result of the contributions coming from the 5d - ²F_{7/2} electronic transition in the Ce³⁺ ions incorporated in SrF₂ lattice (Singh, Lakshminarayana, Sharma, Dao, Chen, Wada, Takeda and Nagao, 2015).

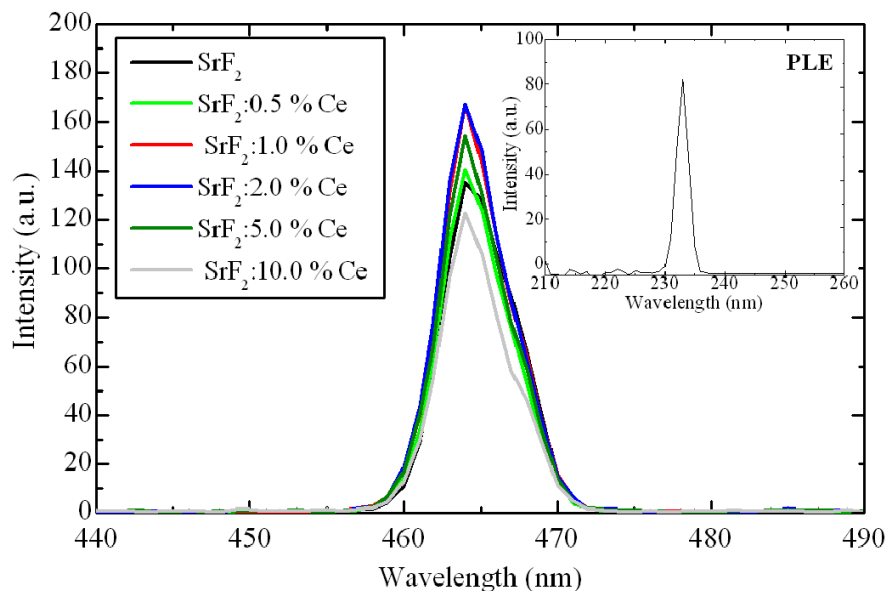


Figure 3. PL spectra of SrF₂ and SrF₂:xCe³⁺ (x=0.5%, 1.0%, 2.0%, 5.0%, 10.0%) nanoparticles. Inset shows the photoluminescence excitation (PLE) spectrum of SrF₂ nanoparticles dispersed in methanol.

In order to examine the gamma ray energy response, synthesized SrF_2 and $\text{SrF}_2:1\% \text{Ce}^{3+}$ nanoparticles were incorporated into epoxy (EPOTEK-301-2FL) matrix. Fabricated composite samples were coupled with PMT tube and before measurements optically shielded assembly was left at room temperature for 24 hours to eliminate the fluorescence effect.

Gamma ray energy spectrums of the fabricated composite samples and neat epoxy were collected by directly placing the Am-241, Cs-137, and Co-60 point sources on top of the disc shaped samples. Background and activity corrections of the collected energy spectrums were performed. Beside these, energy spectrums were also normalized with respect to the number of photons released from point sources.

For all samples, full energy photopeaks of the Am-241, Cs-137, and Co-60 point sources could not be observed and hence, energy calibration could not be performed. However, it is known that there is a relation between the gamma ray energy and the channel numbers.

Figure 4 illustrates the gamma ray energy response of the SrF_2 nanoparticles incorporated epoxy matrix nanocomposite. It is clear from this figure that the count rates rise with the increase in the energy of the used point source.

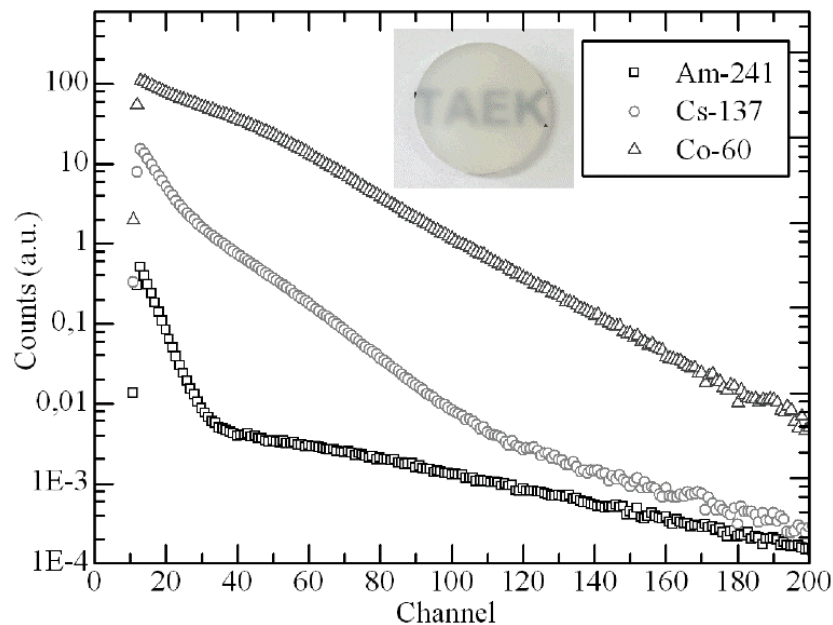


Figure 4. Gamma ray energy spectrums of SrF_2 nanoparticles – epoxy matrix composite (Inset shows the photograph of the fabricated composite sample).

Figure 5 shows the gamma ray energy spectrums of the nanocomposites loaded with either SrF_2 or $\text{SrF}_2:1\% \text{Ce}^{3+}$ nanoparticles and neat epoxy for comparison. It is clear from this figure that neat epoxy has also scintillation properties. Nevertheless, for nanocomposite samples, which are more translucent as compared to neat epoxy, collected count rates are higher in low, medium and high channel numbers depending on the point source used. For the samples irradiated with low energy point source Am-241 which has 59,54 keV gamma line [Figure 5(a)], nanophosphor filled composite samples exhibits higher count rates as compared to that of the neat epoxy at channel numbers lower than 40, whereas for samples irradiated with Cs-137 which has 661,66 keV gamma line [Figure 5(b)] and Co-60 which has 1173,23 keV and 1332,49 keV gamma lines [Figure 5(c)], nanophosphor filled composite samples exhibits higher count rates as compared to that of the neat epoxy at channel numbers 30-120 and 60-200, respectively.

Therefore, in view of the above findings, mentioned channel intervals are thought to be related with the energy of the used point source.

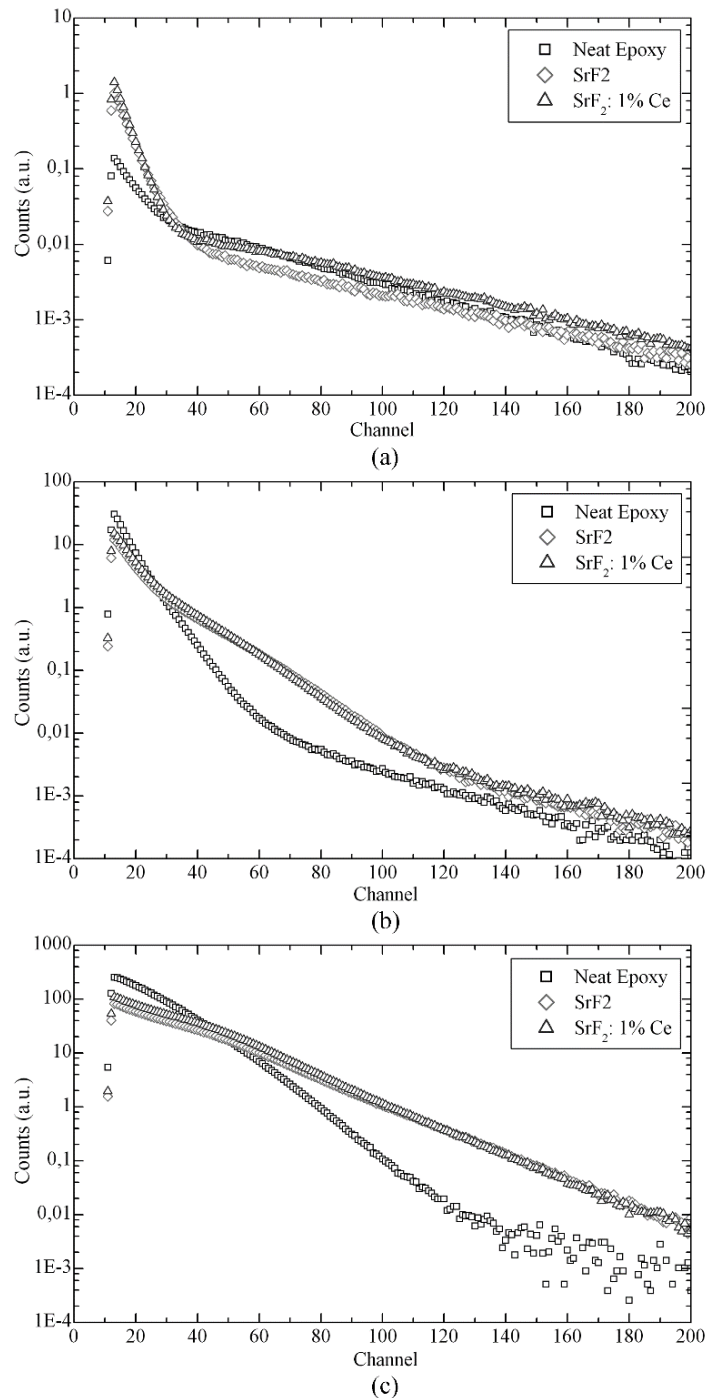


Figure 5. Energy spectrums of epoxy matrix nanocomposites loaded either with SrF₂ or SrF₂:1% Ce³⁺ nanoparticles and neat epoxy irradiated with (a) Am-241, (b) Cs-137 and (c) Co-60 point sources.

The enhancement in gamma ray energy response as a result of the incorporation of nano sized phosphor fillers explicitly reveals the scintillation characteristics of the synthesized nanophosphors. Although further studies should be performed, all these findings infer that

fabricated nanocomposite scintillators show a potential for the energy discrimination of the incident gamma rays and hence identification of radionuclides.

4. Conclusions

Nanoparticles of SrF₂ and SrF₂:xCe (x= 0.5%, 1.0%, 2.0%, 5.0%, 10.0%) were successfully synthesized using the chemical co-precipitation method and the results were comparable in the literature. Although all synthesized nanoparticles show photoluminescence characteristics with an excitation and emission peaks centered at 232 nm and 464 nm, highest luminescence intensity is observed for SrF₂:1%Ce and SrF₂:2%Ce nanophosphors. Gamma ray responses of SrF₂ and SrF₂:1% Ce nanoparticles incorporated epoxy matrix composite samples were determined using Am-241 (1 µCi), Cs-137(0.49 µCi), and Co-60(0.42 µCi) point sources. Although, photopeaks of the Am-241, Cs-137, and Co-60 point sources could not be observed, these fabricated composite scintillators show a potential for energy discrimination of the gamma rays and hence identification of the radionuclides due to the fact that count rates collected for the nanocomposite samples are higher as compared to that of the neat epoxy in different intervals of channel numbers depending on the used point source energy.

5. Acknowledgments

This work was supported by Turkish Atomic Energy Authority (TAEA) (Project No: A3.H3.P1.05).

6. References

- 1) Canning, A., Chaudhry, A., Boutchko, R., Gronbech-Jensen, N. (2010). First-principles studies of luminescence in Ce doped inorganic scintillators. *Physical Review B*, 83, 115-125. Doi: 10.1103/Physical Review B.83.125115.
- 2) De Haas, J. T. M., Dorenbos, P. (2008). Advances in yield calibration of scintillators. *IEEE Transactions on Nuclear Science*, 55, 1086-1092. Doi: 10.1109/TNS.2008.922819.
- 3) Guss, P., Guise, R., Yuan, D., Mukhopadhyay, S., O'Brien, R., Lowe, D., Kang, Z., Menkara, H., Nagarkar, V. V. (2013). Lanthanum halide nanoparticle scintillators for nuclear radiation detection. *Journal of Applied Physics*, 113, 064303/1-064303/6. Doi: 10.1063/1.4790867.
- 4) Jin, Y., Qin, W., Zhang, J. (2008). Preparation and optical properties of SrF₂:Eu³⁺ nanospheres. *Journal of Fluorine Chemistry*, 129, 515-518. Doi: 10.1016/j.jfluchem.2008.03.010.
- 5) Rogers, T., Han, C., Wagner, B., Nadler J., Kang, Z. (2011). Synthesis of luminescent nanoparticle embedded polymer nanocomposites for scintillation applications. *MRS Proceedings*, 1312, 355-360. Doi: 10.1557/opl.2011.123.
- 6) Shendrik, R. Y., Radzhabov, E. A., Nepomnyashchikh, A. I. (2013). Scintillation properties of SrF₂ and SrF₂:Ce³⁺ crystals. *Technical Physical Letters*, 56, 58-61. Doi: 10.1134/S1063785013070109.
- 7) Shendrik, R. Y., Radzhabov, E. A. (2012). Energy transfer mechanism in Pr-doped SrF₂ crystals. *IEEE Transactions on Nuclear Science*, 59, 2089-2094. Doi: 10.1109/TNS.2012.2190146.
- 8) Shendrik, R. Y., Radzhabov, E. A. (2010). Temperature dependence of Ce³⁺ and

Pr³⁺ emission in CaF₂, BaF₂, SrF₂. IEEE Transactions on Nuclear Science, 57, 1295-1299.

9) Singh, S., Lakshminarayana, G., Sharma, M., Dao, T. D., Chen, K., Wada Y., Takeda T., Nagao, T. (2015). Excitation induced tunable emission in Ce³⁺/Eu³⁺ codoped BiPO₄ nanophosphors. J. Spectrosc., 1-10. Doi: 10.1155/2015/493607.

10) Patterson, A. L. (1939). The Scherrer formula for X-Ray particle size determination. Physical Review, 56, 978-982. Doi: 10.1103/Physical Review, 56.978.

11) Yagoub, M. Y. A., Swart, H. C., Noto, L. L., Bergman, P., Coetsee, E. (2015). Surface characterization and photoluminescence properties of Ce³⁺, Eu co-doped SrF₂ nanophosphor. Materials, 8, 2361-2375. Doi: :10.3390/ma8052361.